On the Importance of Benchmarking the Gas-Phase Pyrolysis Reaction in the Oxidative Dehydrogenation of Propane

Journal Article

Author(s):
Nadjafi, Manouchehr; Cui, Yifan; Bachl, Marlon; Oing, Alexander; Donat, Felix; Luongo, Giancarlo; Abdala, Paula Macarena; Fedorov, Alexey; Müller, Christoph R.

Publication date:
2023-05-05

Permanent link:
https://doi.org/10.3929/ethz-b-000609685

Originally published in:
ChemCatChem 15(9), https://doi.org/10.1002/cctc.202200694

Funding acknowledgement:
180544 - NCCR Catalysis (phase I) (SNF)

ChemCatChem

Research Article
doi.org/10.1002/cctc.202200694

Chemistry Europe
European Chemical Societies Publishing

www.chemcatchem.org

On the Importance of Benchmarking the Gas-Phase Pyrolysis Reaction in the Oxidative Dehydrogenation of Propane

Manouchehr Nadjafi,[a] Yifan Cui,[a] Marlon Bachl,[a] Alexander Oing,[a] Felix Donat,[a] Giancarlo Luongo,[a] Paula M. Abdala,[a] Alexey Fedorov,*[a] and Christoph R. Müller*[a]

The oxidative dehydrogenation of propane (ODP) proceeds catalytically on a gas-solid interface (heterogeneous reaction) and/or in the gas phase (homogeneous reaction) via a radical chain process. ODP may therefore combine interrelated contributions from the heterogeneous dehydrogenation and gas-phase reactions, which can be initiated by a catalyst. This study demonstrates that relatively high propene and ethene selectivities (ca. 80% and 10%) and propane conversions (*viz.*, 10% at 500 °C) can be achieved with an empty quartz reactor, which is comparable to the performances of state-of-the-art ODP catalysts (boron-based or supported VO_x). Optimization of the post-catalytic volume of a h-BN catalyst bed tested at 490 °C allows to increase the conversion of propane from 9% to 15% at a propene selectivity of 77%, highlighting this parameter as an important variable for improving catalytic ODP performances.

Introduction

Propene, a key building block for the production of polymers and chemicals, can be produced via the oxidative dehydrogenation of propane [ODP, Equation (1)].[1] Advantages of ODP over conventional, industrially implemented non-oxidative propane dehydrogenation (PDH) include full equilibrium propane conversion, lower reaction temperatures (ca. 500 °C compared to >600 °C), and reaction exothermicity.[2–4] ODP catalysts typically do not deactivate with time on stream (TOS) as little or no coke is formed due to the co-feeding of oxygen. However, a key disadvantage of ODP that hinders its commercialization is the low propene selectivity at high propane conversions (>20%) due to over oxidation of propane/propene, resulting in low propene yields.[2–10]

$$C_3H_8 + 0.5\ O_2 \rightarrow C_3H_6 + H_2O\ (\Delta H^0_{298K} = -117\ kJ\,mol^{-1}) \quad (1)$$

Supported VO_x catalysts have been among the most actively researched materials for ODP in the past decades.[4,6, 11] More recently, boron-based materials have emerged as catalysts that give higher propene selectivities when compared to a VO_x-based catalyst at similar propane conversions.[12–14] The current state-of-the-art ODP catalyst is hexagonal boron nitride, h-BN, which yields propene with 79% selectivity at 14% propane conversion at 490 °C.[15] Other boron-based materials show a comparable performance for ODP.[16,17]

Although several studies have indicated that the ODP performance of V- and B-based catalysts is governed by a combination of surface and gas-phase reactions,[17–22] the exact contribution from the gas-phase reaction (either catalytically or non-catalytically initiated) is understood less, especially at low reaction temperatures (<510 °C).[23–26] Radical species desorbed from the surface of a catalyst can initiate gas-phase ODP reactions, influencing thereby the product distribution as compared to the purely heterogeneous or purely homogeneous gas-phase reaction (oxidative pyrolysis of propane).[18,19,21,22,27–31] Such desorbed species likely include organic radicals similar to those detected by electron paramagnetic resonance (EPR) spectroscopy in reactions of propene over Bi_2O_3 (allyl radicals),[32] or methane over MgO.[33] An additional important but frequently overlooked parameter, is the size of the empty reactor volume downstream of the catalytic bed, i.e., the post-catalytic volume. For example, in the partial oxidation of propene using molecular oxygen at a constant gas-catalyst contact time, the selectivities to acetaldehyde and propene oxide increased while the acrolein selectivity decreased when increasing the post-catalytic volume.[23] For the catalytic oxidation of propene over Mo-based catalysts, increasing the post-catalytic volume gave a higher propene conversion and product selectivity to propene oxide, acetaldehyde and carbon dioxide.[34,35] Furthermore, it has been shown that the oxidation of hydrocarbons, initiated by free radicals, proceeds in the post-catalytic volume,[36] hence its size affects product selectivity in ODP.[19,37]

Indeed, ODP experiments using a V–Mg–O catalyst and reactors with the post-catalytic volume filled with quartz chips

[a] Dr. M. Nadjafi, Y. Cui, M. Bachl, A. Oing, Dr. F. Donat, G. Luongo, Dr. P. M. Abdala, Dr. A. Fedorov, Prof. Dr. C. R. Müller
Department of Mechanical and Process Engineering
ETH Zürich,
Leonhardstrasse 21
CH-8092 Zürich (Switzerland)
E-mail: fedoroal@ethz.ch
muelchri@ethz.ch

Supporting information for this article is available on the WWW under https://doi.org/10.1002/cctc.202200694

(which are generally effective in quenching free radicals) showed a lower propane conversion (trends in propene selectivity varied with reaction temperature) relative to experiments without quartz chips, indicating that the post-catalytic volume influences the extent of the heterogeneous-homogeneous and homogenous ODP reactions.[18,19] Recent ODP studies using h-BN suggest that also for this catalytic system the overall performance has contributions from both heterogeneous and catalytically initiated gas-phase reactions through free radicals (such as $C_3H_7^{\bullet}$ and $HOO^{\bullet}$) desorbing from the h-BN surface and reacting in the void volume between the catalyst particles.[17,20–22,38,39] That being said, our understanding of the contribution of the gas-phase reaction in heterogeneously catalyzed ODP processes to the overall propane conversion and product selectivity is still incomplete.[18,19,40–43] For instance, a recent ODP study on boron isolated in a zeolitic framework reported 55% propene and 26% ethene selectivity at a 41% propane conversion at 560 °C.[44] This performance has been ascribed solely to the activity of the zeolite catalyst in the heterogeneous ODP reaction and it appears that the contribution of gas-phase reactions at temperatures <580 °C has been neglected. Yet the importance of homogeneous gas-phase reactions in the oxidative dehydrogenation of propane at temperatures exceeding ca. 550 °C has been often reported.[24,30,45–47] We show below that the gas-phase reactions contribute substantially to the ODP activity for temperatures >460 °C, whereby their extent depends on the gas hourly space velocity (GHSV), the exact temperature and impurities in the quartz reactors used. Our results are generally consistent with the studies on oxidative pyrolysis of ethane and butane that provided yields of olefins comparable to that of the catalytic oxidative dehydrogenation.[48–50]

Here, to benchmark the impact of the gas-phase reactions on the propane conversion and propene selectivity, we evaluate the influence of the following variables on the non-catalytic gas-phase reaction between propane and oxygen (oxidative pyrolysis of propane): (i) GHSV (16–4500 h^{-1}), (ii) propane to oxygen ratio (from 4:1 to 1:2), (iii) reaction temperature (450–650 °C), (iv) the presence of a filling material and its type (quartz beads, SiC, or quartz wool), (v) reactor design (U-shaped or straight tube), (vi) temperature distribution (reactor placed in a fluidized bed or in a tubular furnace), (vii) the size of the post-catalytic volume, and (viii) the impurities in quartz reactors (reactors from several different suppliers are compared; experiments in i)–vii) were performed in the quartz reactors that have yielded the lowest conversions in the low temperature (450 °C) conditions, *vide infra*). We first discuss the results of the oxidative pyrolysis of propane in an empty quartz tube reactor as a function of temperature and propane to oxygen ratio. Subsequently, we demonstrate that the propane conversion increases by a factor of up to three when increasing the post-catalytic volume from 0 cm^3 to 6.8 cm^3 for a h-BN catalyst while keeping the temperature constant (500 °C). The complete data set of our study is presented in the supporting information file. We note that in some cases the carbon balance is less than 95%, which is explained by the formation of organic oxygenates that are not detected by our GC-FID/TCD used.

Results and Discussion

Non-catalytic ODP. In what follows, we discuss selected experimental data to illustrate that low-temperature homogeneous ODP can provide olefin yields comparable with those of the state-of-the-art heterogeneous catalysts. Using an empty quartz reactor (ID = 15 mm) at 510 °C and a propane to oxygen ratio of 2:1, propene and ethene are produced with selectivities of 74.2% and 12.0%, respectively, at 15.1% propane conversion (Figure 1 and Table 1, entry 1). This result is comparable to the performance of the h-BN catalyst that yields propene and ethene selectivities of 79% and 12%, respectively, at 14% propane conversion at 490 °C (Figure 1 and Table 1, entry 2).[15] A catalyst containing boron in a zeolite framework has been reported to give, at 540 °C and a propane to oxygen ratio of 1:1, propene and ethene selectivities of 55.4% and 27.2% at 23.8% propane conversion (Figure 1 and Table 1, entry 3; selectivity reported among all products).[44] At 540 °C and when using C_3H_8:O_2 ratio of 1:1 in an empty quartz reactor (ID = 10 mm), we obtained propene and ethene selectivities of 68.2% and 18.4%, respectively, at a propane conversion of 25.9% (Table 1, entry 4).

At C_3H_8:O_2 = 2:3 and at various reaction temperatures (straight quartz reactor), we obtain a lower propene yield than the values reported for edge-hydroxylated h-BN (propene and ethene selectivities of, respectively, 80.2% and 10.7% at 20.6% propane conversion and at 530 °C, see Figure 1 and Table 1, entry 5).[36] However, increasing the propane to oxygen ratio to 2:1 and using an empty U-shaped quartz reactor heated in an

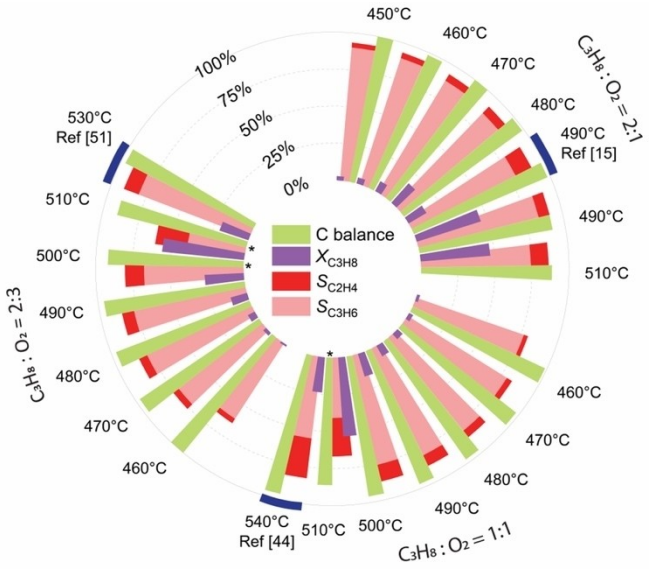

Figure 1. Comparison of the oxidative pyrolysis of propane in an empty quartz reactor (ID = 15 mm, 42 ml min^{-1} total flow rate) and the ODP performance of state-of-the-art boron-based catalysts using different propane to oxygen ratios and temperatures. Marked with asterisks are reactions showing carbon balance lower than 95–97%. Here and below, note that as we report selectivity among the quantified products (see SI for details), reactions with lower carbon balances would consequently have lower selectivities to quantified products if all products are taken into account for the calculation of selectivities.

Table 1. Comparison of the oxidative pyrolysis of propane in empty quartz reactors to the ODP performance of state-of-the-art B-based catalysts. Selectivity values obtained in this work are reported as selectivity based on the quantified products.

Entry	Temp.[°C]	Catalyst	X_{C3H8} [%]	S_{C3H6} [%]	S_{C2H4} [%]	C balance [%]	I.D. [mm]	Reactor shape	Total flow [ml min^{-1}]	C_3H_8:O_2: inert	GHSV[a]/WHSV[b] [h^{-1}]	Ref.
1	510	–	15.1	74.2	12.0	97.0	15	Straight	42	2:1:4	65.3	This study
2	490	h-BN	14.0	79.0	12.0	98.0	9.0	Straight	40	6:3:11	10.6	[15]
3	540	B–S1[c]	23.8	55.4	27.2	96.0	7.4	Straight	30	1:1:8	7.1	[44]
4	540	–	25.9	68.2	18.4	93.2	10	Straight	42	1:1:5	147	This study
5	530	BNOH	20.6	80.2	10.7	97	6	Straight	192	2:3:7	37.6	[51]
6	500	–	21.0	79.0	15	98.1	8	U-shaped	21	2:1:4	188	This study
7	450	–	1.1	90.1	3.3	99.5	15	Straight	52	2:1:4	80.3	This study

[a] Gas hourly space velocity ($L_{C3H8}L_{reactor}^{-1}h^{-1}$). [b] Weight hourly space velocity ($kg_{C3H8}kg_{cat}^{-1}h^{-1}$). [c] –B[OH…O(H)–Si]$_2$ in a borosilicate zeolite.

isothermal fluidized bed yields comparable propene and ethene selectivities of, respectively, 79% and 15% at 21% propane conversion but at a lower temperature of 500 °C (Table 1, entry 6). Likely, the key difference between the results obtained in the straight and U-shaped quartz reactors is the lower temperature gradient in the U-shaped reactor immersed in the fluidized bed (Figure S7). To summarize, the data obtained in empty quartz reactors demonstrate that the oxidative pyrolysis of propane, under optimized conditions, yields performances that can be on par with those of state-of-the-art boron-based ODP catalysts.

The propane conversion rate ($-r_{C3H8}$) in an empty quartz reactor (ID = 15 mm) and at differential propane conversions (< 10%) gives an apparent reaction order for the propane concentration of 2.2 ± 0.1 (Figure S54, $-r_{C3H8} = A \times P_{C3H8}^{2.2}$). It has been argued that the second order rate dependence on the propane partial pressure is an indication of the simultaneous occurrence of surface and gas-phase mechanisms.[22] Therefore, quartz may contain surface species that not only quench but also produce radical species. For instance, the activity of quartz in the conversion of para-hydrogen to ortho-hydrogen and hydrogen-deuterium scrambling was attributed to surface sites that formed upon the thermal removal of hydroxyl groups from the quartz surface.[52]

To investigate the role of the thermocouple in quenching or generating radical species, we compared set-ups with and without an internal thermocouple under conditions of oxidative pyrolysis. For an identical set-temperature and reaction conditions (ID = 10 mm, C_3H_8:O_2:N_2 = 12:6:24) and as long as the oxygen conversion is less than 100%, higher propane conversions are obtained in all experiments in which the temperature is controlled using an external thermocouple (Figure S8). For example, at 490 °C, when the temperature is controlled by an external thermocouple, a propane conversion of 29.8% is achieved while at the same temperature and using an internal thermocouple, the conversion reaches only 7.7%. This is an indication that gas-phase radicals may be quenched by the thermocouple used. We note that an internal thermocouple placed inside the catalyst bed has been a preferred temperature control method for the boron-based catalysts.[10,27,32] While the influence of the thermocouple in an empty reactor experiment might appear surprising, a typical heterogeneous experiment uses a thermocouple immersed in the middle of the catalyst bed, which may limit its influence.

For all propane to oxygen ratios explored here, we observe an increase in the propane conversion when increasing the temperature (provided the oxygen conversion is < 100%) and this is often (but not always) associated with a decrease in the propene selectivity (Figures S8–S47). As soon as full oxygen conversion is reached, the propane conversion increases more slowly with increasing temperature. High propene selectivity of 90.1% (ethene selectivity 3.3%) is achieved in an empty straight quartz reactor at 1.1% propane conversion at 450 °C (Table 1, entry 7; see Tables in the SI for carbon balance data to estimate the selectivities among all reaction products. In cases for which the carbon balance is lower than 95–97%, the selectivity for the quantified products, as specified in the SI, will be higher than selectivity obtained when all reaction products are taken into account).

Increasing the GHSV generally results in lower propane conversions and higher propene selectivities (depending on the propane to oxygen ratio). For example, using a propane to oxygen ratio of 2:1 at 480 °C and doubling the GHSV from 32.7 h^{-1} to 65.3 h^{-1} decreases the propane conversion from 10.2% to 3.9% while increasing the propene selectivity from 74.3% to 86.3% (see the SI file for full details). At a constant GHSV and by varying the propane to oxygen ratio, we do not observe a clear trend in the propane conversion and propene selectivity. For instance, at 480 °C and a GHSV of 65.3 h^{-1}, increasing the propane to oxygen ratio from 1:2 to 2:3 to 1:1 and further to 2:1 changes the propane conversion from 1.4% to 5.1%, to 4.7% and further to 3.9%, while the propene selectivity changes from 86.7% to 78.1% to 80.7% and further to 86.3%. However, a stoichiometric propane to oxygen ratio of 2:1 usually yields better results for both propane conversion and propene selectivity.

To evaluate if metal impurities in quartz can affect the ODP reaction, we compared results obtained using reactors from three different suppliers. The quantities of trace impurities in these reactors are listed in Table S54. At a GHSV of 65.3 h^{-1} and

a propane to oxygen ratio of 2:1, the gas-phase reaction initiates at relatively low temperatures and, for instance, at 460 °C the propane conversion was 1.6%, 6.2% and 5.6% in reactors purchased from Heraeus, E-create Technology and proQuartz, respectively (see SI for details). We note specifically that most of the experiments reported in this work, including those that varied the post-catalytic volume, were performed in quartz reactors purchased from Heraeus that showed the lowest conversion (i.e., 1.6%) in the mentioned conditions. Such differences indicate that metal impurities in quartz may indeed influence the gas-phase ODP reaction. Unfortunately, it is challenging to identify which one of the impurities in the quartz triggers the gas-phase reaction due to the large number of various impurities (in ppm amounts) contained in the reactors utilized. We also note that the ODP results obtained using the U-shaped reactor may also depend on the composition of quartz reactor used.

Catalytic ODP. Further experiments aim to maximize the catalytic propane conversion and propene selectivity at low temperatures (< 510 °C) by combining catalytic and gas-phase reactions in a straight quartz tube reactor, as it is the most frequently applied reactor design. To explore the effect of the size of the post catalytic volume on the propene yield, we use h-BN as the catalyst, a reactor of ID = 15 mm and quartz inserts of ID = 12 mm to define the post-catalytic volume (Figure S48). In total, three different post-catalytic volumes are investigated, i.e., ca. 0 cm^3 (where the entire post-catalytic volume is filled with quartz chips), 4.5 cm^3 and 6.8 cm^3. The ODP was performed at 490 °C and $C_3H_8:O_2 = 2:1$ (most commonly used ratio).[2,5] Increasing the size of the post-catalytic volume from 0 cm^3 to 4.5 cm^3 and to 6.8 cm^3, the conversion of propane increases from 9.2% to 15.1% and to 16.4% at propene selectivities of 77.3%, 77.2%, and 74.6%, respectively, while the ethene selectivities increase from 11.1% to 13.6% and to 14.2% (Figures 2 and S48). This result suggests that radicals desorbed from the surface of h-BN, react further with other species in the gas-phase, increasing the conversion of propane (at a given temperature and for an oxygen conversion < 100%). When reaching full oxygen conversion, the conversion of propane does not change significantly when increasing the temperature (up to 550 °C, i.e. the highest temperature used in these experiments), irrespective of the size of the post-catalytic volume. At 500 °C and maintaining a $C_3H_8:O_2$ ratio of 2:1 (h-BN catalyst), the conversion of propane increases from 12.2% to 22.2% and to 38.6% when increasing the post-catalytic volume from 0 cm^3 to 4.5 cm^3 and to 6.8 cm^3 (Figure 2 and S48). However, the combined selectivity to propene and ethene decreases from 87.6% for h-BN in a reactor with a post-catalytic volume of 0 cm^3 to 86.5% and to 70.6% for post-catalytic volumes of 4.5 cm^3 and 6.8 cm^3, respectively.

Interestingly, at 500 °C the conversions of propane obtained in configurations with a post-catalytic volume > 0 cm^3 are notably higher than the sum of the catalytic conversion (12.2% with 0 cm^3 post-catalytic volume) and the pure gas-phase conversions (oxidative pyrolysis of propane) obtained with the respective inserts inside the quartz reactor (i.e., 4.6% and 2.7% for 4.5 cm^3 and 6.8 cm^3 empty tube insert volumes, respectively). This observation is indicative of the presence of a heterogeneous-homogeneous reaction mechanism for ODP when using h-BN catalyst (Figures 3 and S48).[33–35]

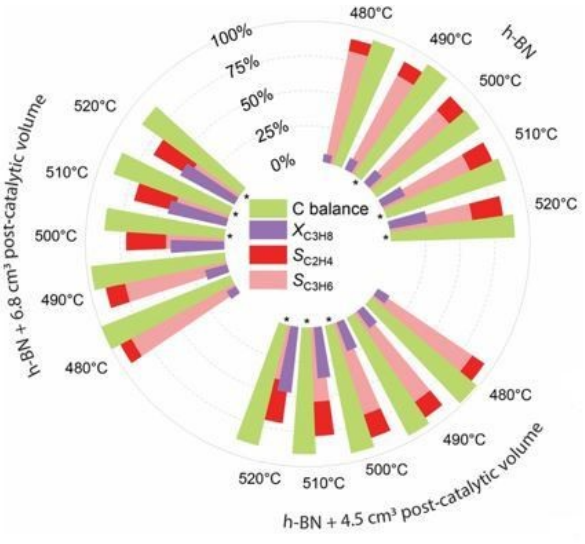

Configuration	Temp. (°C)	X_{C3H8}(%)	S_{C3H6}(%)	S_{C2H4}(%)	C balance (%)
h-BN	480	5.8	81.7	8.9	93.8
	490	9.2	77.3	11.1	95.5
	500	12.2	73.8	13.8	89.0
	510	18.3	68.4	17.5	90.1
	520	27.7	59.9	22.4	89.3
h-BN + 4.5 cm^3 post-catalytic volume	480	9.9	83.0	10.6	98.5
	490	15.1	77.2	13.6	95.7
	500	22.2	69.1	17.4	93.4
	510	36.8	53.5	24.7	91.0
	520	47.5	39.5	30.5	89.1
h-BN + 6.8 cm^3 post-catalytic volume	480	7.6	84.0	9.0	99.9
	490	16.4	74.6	14.2	96.7
	500	38.6	42.2	28.6	86.6
	510	43.1	39.1	29.7	88.6
	520	44.2	38.2	30.0	87.1

Figure 2. ODP performances when a catalytic process using h-BN is combined with gas-phase reactions (Figure S48). Reactor (straight quartz tube of ID = 15 mm, insert tube ID = 12 mm) filled with 225 mg catalyst mixed with 450 mg SiC, $C_3H_8:O_2:N_2 = 2:1:4$, 42 ml min^{-1} total flow rate. A K-type thermocouple was placed inside the catalyst bed for all experiments and the catalyst bed was in the center of the vertical tubular furnace. Marked with asterisks are reactions showing carbon balance lower than 95–97%.

A comparison between the ODP results obtained when using h-BN with and without a post catalytic volume to the oxidative pyrolysis of propane performed under similar conditions using an empty quartz reactor suggests a greater contribution to product formation from oxidative pyrolysis over catalytic ODP (Figure 3). This may be due to the different nature of the propyl radicals involved, that is, mainly *n*-propyl radicals desorb from the h-BN surface and these radicals favour formation of ethene and CO_x whereas propyl radicals generated during the gas-phase propagation are mainly iso-propyl radicals that favour selective ODP.[33–35,53] In addition, the activation energy of ODP over h-BN was lower than the activation energy of oxidative pyrolysis in an empty quartz reactor (ID = 15 mm, 215 kJ mol^{-1} and 261 kJ mol^{-1}, respectively, Figure S49). The higher yield in a gas phase reaction was ascribed previously to the role of h-BN in quenching $HOO^{\bullet}$ radicals.[22] The surface area

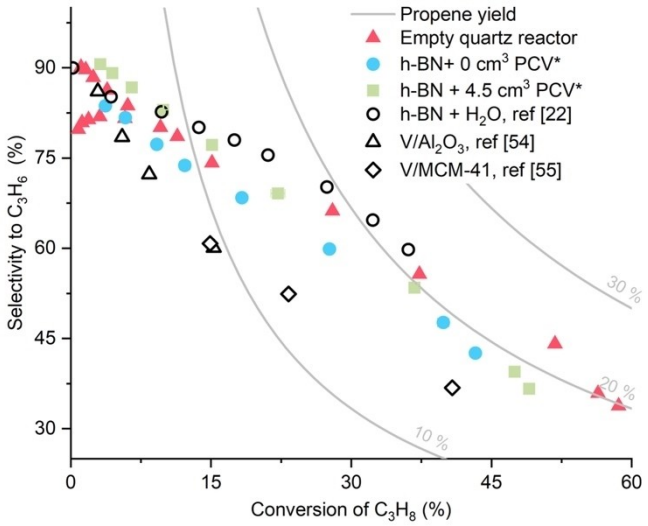

Figure 3. Propene selectivity as a function of propane conversion using state-of-the-art ODP catalysts based on h-BN or supported VO_x, compared to the catalytic and non-catalytic performances obtained in this work. A quartz reactor with ID = 15 mm was used either empty or filled with a catalyst (225 mg h-BN mixed with 450 mg SiC), $C_3H_8:O_2:N_2 = 2:1:4$, 42–52 ml min^{-1} total flow rate. (* PCV stands for post catalytic volume).

to volume ratio of h-BN is ca. three orders of magnitude higher than that of the empty quartz reactor (ID = 15 mm, L = 200 mm) explaining the different extends of radical quenching to radical propagation for h-BN and the empty quartz reactor.

Conclusion

Results presented herein highlight the importance of the oxidative pyrolysis of propane and heterogeneous-homogeneous reactions in ODP for a broad range of temperatures and GHSVs. Using an empty quartz reactor (ID = 15 mm, GHSV = 80.3 h^{-1}) at 490 °C and a propane to oxygen ratio of 2:1, a propane conversion of 30 % at a total olefin selectivity of 82.6 % (64.1 % propene and 18.5 % ethene) is achieved. Moreover, by combining catalytic (heterogeneous) and gas-phase reactions, a substantial increase in the propane conversion is obtained at reaction temperatures below 510 °C, as radicals desorbed from h-BN react further in the gas-phase. This observation is consistent with the co-existence of a heterogeneous-homogeneous mechanism (i.e., catalytically initiated gas-phase reaction),[16] in addition to heterogeneous (catalytic) and homogeneous (gas-phase) reactions in ODP using a h-BN catalyst. Note that the surface of quartz may play a similar role to h-BN and provide radical species for the gas-phase reaction. Overall, the experimental results of this study provide evidence that robust conclusions concerning the contribution of the heterogeneously catalyzed ODP reactions can be drawn only when comparing results of catalyzed and blank control experiments,[56] as oxidative pyrolysis in an empty quartz reactor can yield comparable performances relative to both catalytic and combined catalytic and catalytically initiated gas-phase ODP reactions.

Experimental Section

Reaction setup 1. U-shaped quartz reactors (Heraeus, Germany) with internal diameters of 4 and 8 mm, 225 mm height, and 2 mm wall thickness have been used. A reactor was placed inside a bed of alumina sand (Kuhmichel, 300–425 μm) that was fluidized by compressed air (14–19 L min^{-1}, $U_{mf} \approx 0.169$–0.178 m s^{-1}). Only the bottom part of the reactor (ca. 55 mm) was immersed inside the fluidized bed, yielding effective reaction volumes (i.e., the volume of the empty space of the reactor immersed inside the fluidized bed) of ca. 1.6 and 6.1 cm^3 for the U-shaped reactors with ID 4 mm and 8 mm, respectively. The temperature gradient along this effective reaction volume was always less than 5 °C (as determined in a N_2 flow at 550 and 600 °C, Figure S1). For the oxidative pyrolysis of propane (> 99.95 %, Carbagas), the temperature was varied between 450–650 °C in increments of 50 °C. Synthetic air, nitrogen, and propane were flown through the reactor using Bronkhorst mass flow controllers (MFC) that were calibrated prior to the experiments using a calibration flowmeter (ANALYT-MTC) at 25 °C. A total flow of 9–120 ml min^{-1} was used to achieve different gas hourly space velocities (GHSV) while the propane to oxygen ratio was changed from 1:1 to 2:1, and 4:1. Off-gases were analyzed using a compact gas chromatograph (GC, Global Analyzer Solutions) every three minutes. Prior to gas analysis water vapor was condensed from the gas stream using a glass condenser. In the GC, H_2, O_2, N_2, and CO were separated using a Molsieve 5 A (5 m × 0.32 mm) connected to an RT–Q-BOND column (7 m and 3 m × 0.32 mm) while the CO_2 was separated using two RT–Q-BOND columns in series (10 m and 3 m × 0.32 mm) and quantified by two thermal conductivity detectors (TCD). Hydrocarbons were separated using an Rtx-5, 3u (15 m × 0.32 mm) column and detected by a flame ionization detector (FID). For the quenching experiments, SiC (Alfa Aesar, 46 grit particles) or quartz beads (Pyromatics, 0.5–1 mm) were used. Here, the U-shaped reactors were filled to three different levels with quartz chips or SiC to study their effectiveness in quenching gas-phase radicals at elevated temperatures.

Reaction setup 2. Two straight quartz reactors (Heraeus, Germany) with internal diameters of 10 and 15 mm, 360 mm length, have been used. A reactor was heated in a 200 mm height cylindrical furnace using a PID Microactivity-Effi (PID ENG&TECH) integrated reactor setup. The furnace and all of the valves were inside a hot box that was kept at 150 °C during all experiments irrespective of the reaction temperature used. The temperature profile along the furnace was measured using two K-type thermocouples. One thermocouple was fixed inside the straight quartz reactor in the center of the furnace and the second thermocouple was placed outside of the reactor and inside the furnace in the center of the furnace. Only a minor temperature difference was found between the temperatures measured inside and outside of the reactor. The outside thermocouple was used to obtain the temperature profile in the furnace with respect to the center of the reactor. Flow rates of propane, air, and nitrogen were controlled using Bronkhorst MFCs to achieve a total flow rate of 10.5–52 ml min^{-1} with different propane to air ratios (2:1, 1:1, 2:3, and 1:2) within a temperature range of 450–550 °C in increments of 10 °C. Off-gases were analyzed by a Clarus 580 GC (PerkinElmer) equipped with a methanizer to increase the precision of the CO_x measurement. The PID setup was equipped with a liquid-gas separator that is cooled thermoelectrically to condense the water before entering the GC. All carbon products were separated by a HP Plot Q Restek column (30 m × 0.32 mm) and analyzed by an FID. H_2, N_2, and O_2 were separated by

a ShinCarbon ST 80/100 Restek column (3 m × 1 mm) and analyzed by a TCD. Every 16 min a data point was collected by the GC, beginning 10 min after the start of the reaction while the first data point was always collected after 10 min after the start of the reaction. The carbon balance depended on the reaction parameters and varied between 80 to 100%. For the gas-phase quenching experiments in the straight quartz reactors, quartz beads, SiC, and quartz wool were used. To fully fill the straight quartz reactor (ID 10 mm), an amount of 22.8 g, 4.367 g, and 32.51 g of quartz beads, quartz wool, and SiC were used, respectively.

Catalytic experiments. Reaction setup 2 was used for catalytic tests with hexagonal boron nitride (h-BN, 99.5%, Alfa Aesar). h-BN powder was first pressed into a pellet, crushed using a pestle and a mortar, and then sieved into 180–350 μm size. Sieved h-BN (225 mg) was mixed with SiC in a 1:2 mass ratio and placed between two thin quartz wool plugs (0.6–0.9 cm) while the rest of the reactor was filled with quartz beads to quench gas-phase reactions. Different quartz inserts (see SI file for sketches and images) were placed right after the catalytic bed to investigate the effect of the size of the post catalytic volume on the observed performance of the catalyst.

A straight quartz reactor inside a vertical tubular furnace is considered as a representative setup of typical reactor systems used in research laboratories. By using a hollow quartz insert inside the reactor tube and varying the total flow rate in reaction setup 2 it was possible to achieve GHSVs up to 4082.7 h^{-1}. Except for the inserts, the rest of the reactor was filled with quartz beads to quench gas-phase reactions. To ensure a good separation between the quartz beads and the post catalytic volume, we used stainless steel metal meshes that were catalytically inactive.

Control experiments showed that while an empty quartz reactor converts propane and oxygen (2:1 ratio, GHSV = 147 h^{-1}) at 550 °C with a propane conversion of 40%, filling the entire reactor volume with quartz beads or SiC reduces the propane conversion to almost negligible values of ca. 2%. Thus, quartz beads and SiC are effective quenchers of the gas-phase reaction, while quartz wool (filling density = 0.154 g ml^{-1}) is less effective and gives propane conversions of 12%.

To evaluate the influence of quartz impurities on the oxidative pyrolysis of propane, we have used quartz reactors from three different producers. Trace element analysis of these reactors, as supplied by the producers, are presented in Table S54.

Acknowledgements

This publication was created as part of NCCR Catalysis (grant number 180544), a National Centre of Competence in Research funded by the Swiss National Science Foundation. Open Access funding provided by Eidgenössische Technische Hochschule Zürich.

Conflict of Interest

The authors declare no conflict of interest.

Data Availability Statement

The data that support the findings of this study are available in the supplementary material of this article.

Keywords: heterogeneous-homogeneous reactions · hexagonal boron nitride · oxidative dehydrogenation of propane · oxidative pyrolysis of propane · surface-initiated gas-phase reaction

[1] E. E. Stangland, *Annu. Rev. Chem. Biomol. Eng.* **2018**, *9*, 341–364.
[2] J. T. Grant, J. M. Venegas, W. P. McDermott, I. Hermans, *Chem. Rev.* **2018**, *118*, 2769–2815.
[3] J. J. H. B. Sattler, J. Ruiz-Martinez, E. Santillan-Jimenez, B. M. Weckhuysen, *Chem. Rev.* **2014**, *114*, 10613–10653.
[4] C. A. Carrero, R. Schlögl, I. E. Wachs, R. Schomaecker, *ACS Catal.* **2014**, *4*, 3357–3380.
[5] T. Otroshchenko, G. Jiang, V. A. Kondratenko, U. Rodemerck, E. V. Kondratenko, *Chem. Soc. Rev.* **2021**, *50*, 473–527.
[6] F. Cavani, N. Ballarini, A. Cericola, *Catal. Today* **2007**, *127*, 113–131.
[7] M. Baerns, O. Buyevskaya, *Catal. Today* **1998**, *45*, 13–22.
[8] C. Boyadjian, K. Seshan, L. Lefferts, A. G. van der Ham, H. van den Berg, *Ind. Eng. Chem. Res.* **2011**, *50*, 342–351.
[9] V. S. Arutyunov, R. N. Magomedov, *Russ. Chem. Rev.* **2012**, *81*, 790–822.
[10] V. S. Arutyunov, *Rev. Chem. Eng.* **2021**, *37*, 99–123.
[11] O. Ovsitser, R. Schomaecker, E. V. Kondratenko, T. Wolfram, A. Trunschke, *Catal. Today* **2012**, *192*, 16–19.
[12] B. Frank, J. Zhang, R. Blume, R. Schlögl, D. S. Su, *Angew. Chem. Int. Ed.* **2009**, *48*, 6913–6917; *Angew. Chem.* **2009**, *121*, 7046–7051.
[13] L. Shi, Y. Wang, B. Yan, W. Song, D. Shao, A.-H. Lu, *Chem. Commun.* **2018**, *54*, 10936–10946.
[14] X. Sun, Y. Ding, B. Zhang, R. Huang, D. S. Su, *Chem. Commun.* **2015**, *51*, 9145–9148.
[15] J. T. Grant, C. A. Carrero, F. Goeltl, J. Venegas, P. Mueller, S. P. Burt, S. E. Specht, W. P. McDermott, A. Chieregato, I. Hermans, *Science* **2016**, *354*, 1570–1573.
[16] J. T. Grant, W. P. McDermott, J. M. Venegas, S. P. Burt, J. Micka, S. P. Phivilay, C. A. Carrero, I. Hermans, *ChemCatChem* **2017**, *9*, 3623–3626.
[17] J. M. Venegas, W. P. McDermott, I. Hermans, *Acc. Chem. Res.* **2018**, *51*, 2556–2564.
[18] K. T. Nguyen, H. H. Kung, *Ind. Eng. Chem. Res.* **1991**, *30*, 352–361.
[19] K. T. Nguyen, H. H. Kung, *J. Catal.* **1990**, *122*, 415–428.
[20] J. M. Venegas, I. Hermans, *Org. Process Res. Dev.* **2018**, *22*, 1644–1652.
[21] P. Kraus, R. P. Lindstedt, *J. Phys. Chem. C* **2021**, *125*, 5623–5634.
[22] J. M. Venegas, Z. Zhang, T. O. Agbi, W. P. McDermott, A. Alexandrova, I. Hermans, *Angew. Chem. Int. Ed.* **2020**, *59*, 16527–16535; *Angew. Chem.* **2020**, *132*, 16670–16678.
[23] C. C. McCain, G. W. Godin, *Nature* **1964**, *202*, 692–693.
[24] M. Y. Sinev, *J. Catal.* **2003**, *216*, 468–476.
[25] R. D. Wilk, N. P. Cernansky, R. S. Cohen, *Combust. Sci. Technol.* **1986**, *49*, 41–78.
[26] M. Cord, B. Husson, J. C. Lizardo Huerta, O. Herbinet, P.-A. Glaude, R. Fournet, B. Sirjean, F. Battin-Leclerc, M. Ruiz-Lopez, Z. Wang, *J. Phys. Chem. A* **2012**, *116*, 12214–12228.
[27] N. R. Altvater, R. W. Dorn, M. C. Cendejas, W. P. McDermott, B. Thomas, A. J. Rossini, I. Hermans, *Angew. Chem. Int. Ed.* **2020**, *59*, 6546–6550; *Angew. Chem.* **2020**, *132*, 6608–6612.
[28] A. M. Love, B. Thomas, S. E. Specht, M. P. Hanrahan, J. M. Venegas, S. P. Burt, J. T. Grant, M. C. Cendejas, W. P. McDermott, A. J. Rossini, I. Hermans, *J. Am. Chem. Soc.* **2019**, *141*, 182–190.
[29] A. Beretta, L. Piovesan, P. Forzatti, *J. Catal.* **1999**, *184*, 455–468.
[30] A. Beretta, P. Forzatti, E. Ranzi, *J. Catal.* **1999**, *184*, 469–478.
[31] M. Xu, J. H. Lunsford, *React. Kinet. Catal. Lett.* **1996**, *57*, 3–11.
[32] W. Martir, J. H. Lunsford, *J. Am. Chem. Soc.* **1981**, *103*, 3728–3732.
[33] D. J. Driscoll, W. Martir, J. X. Wang, J. H. Lunsford, *J. Am. Chem. Soc.* **1985**, *107*, 58–63.
[34] C. Daniel, G. W. Keulks, *J. Catal.* **1972**, *24*, 529–535.
[35] C. Daniel, J. R. Monnier, G. W. Keulks, *J. Catal.* **1973**, *31*, 360–368.
[36] D. J. Driscoll, K. D. Campbell, J. H. Lunsford, *Adv. Catal., Vol. 35* **1987**, pp. 139–186.

[37] V. Vislovskiy, T. Suleimanov, M. Y. Sinev, Y. P. Tulenin, L. Y. Margolis, V. C. Corberán, *Catal. Today* **2000**, *61*, 287–293.
[38] W. P. McDermott, J. Venegas, I. Hermans, *ChemSusChem* **2020**, *13*, 152–158.
[39] X. Zhang, R. You, Z. Wei, X. Jiang, J. Yang, Y. Pan, P. Wu, Q. Jia, Z. Bao, L. Bai, M. Jin, B. Sumpter, V. Fung, W. Huang, Z. Wu, *Angew. Chem. Int. Ed.* **2020**, *59*, 8042–8046; *Angew. Chem.* **2020**, *132*, 8119–8123.
[40] V. R. Choudhary, V. H. Rane, A. M. Rajput, *AIChE J.* **1998**, *44*, 2293–2301.
[41] R. Burch, E. M. Crabb, *Appl. Catal. A* **1993**, *100*, 111–130.
[42] S. K. Layokun, *Ind. Eng. Chem. Process Des. Dev.* **1979**, *18*, 241–245.
[43] C. K. Westbrook, W. J. Pitz, *Combust. Sci. Technol.* **1984**, *37*, 117–152.
[44] H. Zhou, X. Yi, Y. Hui, L. Wang, W. Chen, Y. Qin, M. Wang, J. Ma, X. Chu, Y. Wang, X. Hong, Z. Chen, X. Meng, H. Wang, Q. Zhu, L. Song, A. Zheng, F.-S. Xiao, *Science* **2021**, *372*, 76–80.
[45] L. Leveles, K. Seshan, J. Lercher, L. Lefferts, *J. Catal.* **2003**, *218*, 296–306.
[46] M. Machli, C. Boudouris, S. Gaab, J. Find, A. Lemonidou, J. Lercher, *Catal. Today* **2006**, *112*, 53–59.
[47] N. Pogosyan, M. D. Pogosyan, S. Arsentiev, L. Strekova, L. Tavadyan, V. Arutyunov, *Russ. J. Phys. Chem. B* **2015**, *9*, 231–236.
[48] T. M. Huong, A. Suzuki, T. Mizushima, H. Ohkita, N. Kakuta, *J. Jpn. Pet. Inst.* **2006**, *49*, 71–77.
[49] A. A. Lemonidou, A. E. Stambouli, *Appl. Catal. A* **1998**, *171*, 325–332.
[50] S. A. R. Mulla, O. V. Buyevskaya, M. Baerns, *Appl. Catal. A* **2002**, *226*, 73–78.
[51] L. Shi, D. Wang, W. Song, D. Shao, W.-P. Zhang, A.-H. Lu, *ChemCatChem* **2017**, *9*, 1788–1793.
[52] J. R. Harris, D. R. Rossington, *J. Am. Ceram. Soc.* **1968**, *51*, 511–518.
[53] V. S. Arutyunov, V. I. Savchenko, I. V. Sedov, A. V. Nikitin, R. N. Magomedov, A. Y. Proshina, *Russ. Chem. Rev.* **2017**, *86*, 47.
[54] B. Frank, A. Dinse, O. Ovsitser, E. V. Kondratenko, R. Schomäcker, *Appl. Catal. A* **2007**, *323*, 66–76.
[55] E. V. Kondratenko, M. Cherian, M. Baerns, D. Su, R. Schlögl, X. Wang, I. E. Wachs, *J. Catal.* **2005**, *234*, 131–142.
[56] L. Annamalai, Y. Liu, P. Deshlahra, *ACS Catal.* **2019**, *9*, 10324–10338.

Manuscript received: May 31, 2022
Revised manuscript received: March 2, 2023
Accepted manuscript online: March 14, 2023
Version of record online: April 7, 2023